Journal of the Korean Physical Society, Vol. 65, No. 2, July 2014, pp. 162∼167

Carrier Transport Mechanisms of Hybrid ZnO Nanorod-polymer LEDs

Sungjae Cho, Kyu Seung Lee and Dong Ick Son*
Soft Innovative Materials Research Center, Korea Institute of Science and Technology, Wanju 565-905, Korea

Youngjei Oh and Won Kook Choi†
Interface Control Research Center, Korea Institute of Science and Technology, Seoul 131-791, Korea

Basavaraj Angadi
Department of Physics, Bangalore University, Bangalore - 560 056, India

(Received 14 January 2014)

A hybrid polymer-nanorod (NR) light-emitting diode (LED), consisting of a hole-conducting polymer poly (9-vinyl carbazole) (PVK) and ZnO nanorod (NR) composite, with the device structure of glass/indium-tin-oxide (ITO)/PEDOT:PSS/(PVK + ZnO nanorods)/Al is fabricated through a simple spin coating technique. TEM images shows inhomogeneous deposition and the agglomeration of ZnO NRs, which is explained through their low probability of adsorption on PVK due to two-dimensional structural property. In the current-voltage characteristics, negative differential resistance (NDR) phenomenon is observed corresponding to device structure without ZnO NRs. The carrier transport behavior in the LED device is well described by both ohmic and space-charge-limited-current (SCLC) mechanisms. Broad blue electroluminescence (EL) consisting of two sub peaks, are centered at 441 nm and the other at 495 nm, is observed, which indicates that the ZnO nanorod play a role as a recombination center for excitons. The red shift in the position of the EL compared to that photoluminescence is well explained through band offsets at the heterojunction between the PVK and ZnO NRs.

PACS numbers: 78.55.Et, 78.66.Sq, 78.67.Bf
Keywords: ZnO nanorod, Hybrid polymer-nanorod, Light-emitting diode
DOI: 10.3938/jkps.65.162

I. INTRODUCTION

The advantages of hybird device based on organic-inorganic materials are due to the diversity of organic materials and the high performance electronic and optical properties stem from the inorganic materials [1–3]. Low-dimensional inorganic nano-structured materials, as one of the component materials for such hybrid devices, have attracted great interest these days because of their unique physical and chemical properties [4–7]. Ease of synthesis and precise dimensional control of the inorganic semiconductors along with proper integration into the organic component are the major challenges for the successful fabrication of these hybrid devices.

Various nano-structured inorganic semiconducting materials have been explored for making hybrid light-emitting diodes, but most studies have focused on inorganic nanocrystal (NC)-polymer based devices with quantum dots embedded in a polymer matrix [1–3]. Among these materials, ZnO with a direct band gap of 3.37 eV and a large exciton binding energy of 60 meV at room temperature [8] has been widely investigated for potential applications in ultraviolet nanolaser sources [9], gas sensors [10], solar cells [11], and field emission display devices [12]. In the past years, various methods such as hydrothermal [13], metalorganic chemical-vapor deposition [14], and physical vapor deposition have been adopted to synthesize ZnO nanostructures [15]. Recently, the development of LED devices using hybrid organic materials with synthesized ZnO nanocrystals has been the subject of many studies [16,17]. Although a few electroluminescent devices based on an inorganic ZnO nanocrystal/organic heterostructure have been reported [17–21], studies on electroluminescent device consisting of an hybrid inorganic/organic nanocomposite heterostructure using ZnO nanorods with a simple chemical method of preparation are scarce.

In this work, two-dimensional ZnO nanorods (NRs) were used, as exciton recombination centers to fabricate inorganic-polymer hybrid LEDs by a simple spin-coating technique. The microstructure, carrier transport be-

*E-mail: eastwing33@hanmail.net
†E-mail: wkchoi@kist.re.kr

havior, photoluminescence (PL) and electroluminescence (EL) of the device were studied in detail.

II. EXPERIMENTS

We adopted a simple chemical method to prepare ZnO nanorods and a spin-coating method to deposit an organic-inorganic composite film for the developed EL devices. Patterned ITO glass, supplied by Sunic System, was used as a substrate, and routine chemical cleaning procedure including ultra-sonification in a detergent (trichloroethylene, acetone, and methanol solution) and rinsing with deionized water, was adopted. The ZnO nanorods were preapared as follows. An aqueous solution of 0.5 M $Zn(NO_3)_2$ was mixed with an excessive amount of 2 M $(NH_4)_2CO_3$ solution. The reaction produced an amorphous powder of zinc carbonate hydroxide, $Zn_2(OH)_2CO_3 * xH_2O$ (ZCH), composed of 50nm diameter nanofibers [22]. A mixture of ZCH with NaCl or NaCl-Li_2CO_3 was milled for $12 - 24$ h in a Pulverisette 5 (Fritsch) planetary mill at 700 rpm in a Zr jar with Zr balls. ZnO nanorods (NRs) were grown from the as-prepared powder mixture, with a 0.5 g ZCH/10 g NaCl or a 0.5 g ZCH/9 g NaCl/1 g Li_2CO_3 weight ratio, in an alumina crucible and subjected to heat treatment in a muffle furnace in air at $600 - 700$ °C for $1 - 6$ h. Other experimental procedures are well described elsewhere [23]. These ZnO NRs were used for the fabrication of the LED device.

As a hole transport layer (HTL), a solution prepared by dissolving the ZnO NRs (0.05 wt%) and PVK (1 wt%) in toluene was spun onto a pre-deposited conducting polymer poly(3,4-ethylenedioxythiophene):poly(styrenesulfonate) (PEDOT:PSS) film on an Indium-Tin-Oxide(ITO) /glass substrate acting as a hole injection layer (HIL). Subsequently the film was annealed at 90 °C for 10 minutes to remove the solvent, and showed a sheet resistance of about 15 Ω/square. Finally, as a top cathode, Al layer of 200 nm in thickness, was deposited through a shadow mask by thermal evaporation. For the measurement of the photoluminescence, a He-Cd laser ($\lambda = 325$ nm) was used as an excitation source. Electroluminescence was measured by using a monochromator (Model: DM500) and a photomultiplier (Model: PDS-1) attached to the PL equipment. A current-voltage (I-V) characteristic curve was obtained by using a HP 4284A precision LCR meter at room temperature. A transmission electron microscope (TEM) (Model: STEM/TEM (CM30)) at a acceleration voltage 200 kV was used to investigate the microstructural distribution of ZnO semiconductor NRs in the hybrid polymer - NR composite.

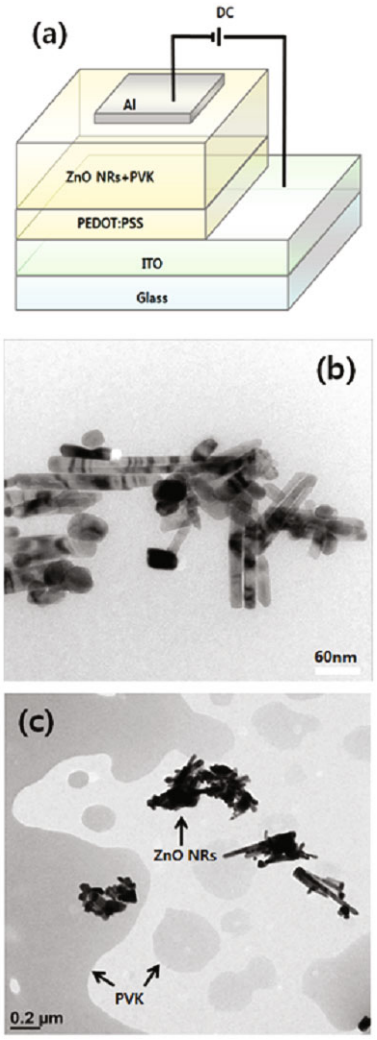

Fig. 1. (Color online) (a) Schematic diagram of LED fabricated using a hybrid PVK polymer and ZnO NRs. Plane-view bright-field Transmission electron microscopy image of (b) ZnO NRs and (c) a hybrid PVK polymer with ZnO NRs.

III. RESULTS AND DISCUSSION

Figure 1(a) illustrates the schematic structure of the hybrid LED with a ZnO NR-PVK polymer structure. Figure 1(b) shows a plane-view bright-field TEM image of the prepared ZnO NRs. The image shows ZnO NRs of about 10 nm in diameter and about $10 \sim 100$ nm in length. Figure 1(c) shows a TEM image of ZnO NRs dispersed in PVK. A careful investigation of Fig. 1(c), show that ZnO NRs are apparently agglomerated, connecting one another, and appear to be distributed non-uniformly throughout the PVK layer. The TEM observation also indicates that the ZnO NRs and the PVK polymer are not mixed together but are separated into two layers. This result is quite different from that previously reported for a CdSe/ZnS-PVK polymer hybrid structure, where core-shell-type CdSe/ZnS NPs were uniformly ad-

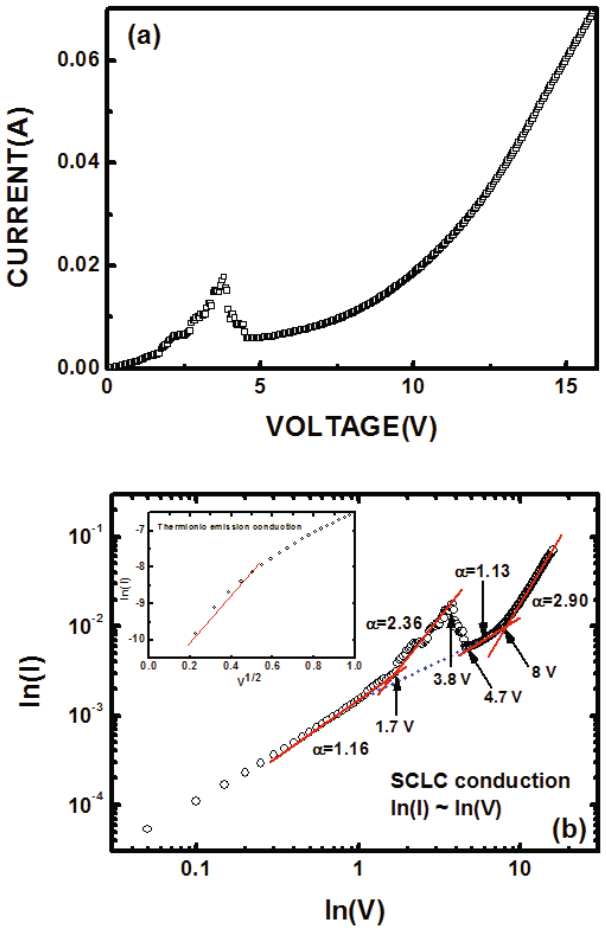

Fig. 2. (Color online) (a) Current-voltage curves for an Al/[ZnO NRs + PVK polymers]/PEDOT:PSS/ITO on glass devices. (b) The fitting plot in the space charge limit current (SCLC) range for Al/[ZnO NRs embedded in a PVK polymers]/PEDOT:PSS/ITO/glass devices. The inset represents the current as a function of the voltage characteristic, obtained by using a fitting of the thermionic emission current.

sorbed on PVK polymer particles [24] and further if small TPBi molecules were mixed with the CdSe/ZnS-PVK hybrid they would have become a consolidated core-shell type hybrid [25]. The contrasting observation in our samples is because of the two dimensional structure of the ZnO NRs used in the present work, which compared to CdSe/ZnS NPs, have a low probability for being adsorbed on PVK polymer particles.

Figure 2(a) shows the current–voltage (I-V) characteristics for the Al/[ZnO nanorods (NRs)]/ PVK/PEDOT:PSS/ITO structure. The $I - V$ curves were obtained by sweeping the applied direct-current voltage bias from −8 V to 8 V. The figure shows an unusual behavior of a negative differential resistance (NDR) at around −4 V and +4 V with a corresponding change in the current from 8 to 5 mA and 17 to 6 mA, respectively. This type of current anomaly, also known as N-type current-voltage characteristics, has been commonly observed in organic light-emitting diodes (OLEDs) comprising small molecules or various kinds of conjugated and non-conjugated polymers, and even dye dopants [31]. Even though the reason for NDR is not precisely known, this phenomenon has been generally ascribed to leakage or short circuits and is a common problem in organic thin films.

In order to examine the carrier transport in hybrid polymer-ZnO NR LEDs, we analyzed the current-voltage characteristic curve by using three basic mechanisms, thermionic emission (TE), space-charge-limited current (SCLC), and Folwer-Nordheim (FN) tunneling [26–28]. Figure 2(b) shows the log-log plot of the I-V curve from 0 to 20 V adapting the SCLC model. The curve could be fitted with four regions showing different linear slopes with the first change of slope occurring at a voltage of 1.7 V. The voltages up to 1.7 V could be fitted with α = 1.16, which means that electrical conduction in this range is governed by ohm's law. As shown in the top inset of Fig. 2(b), where ln(J) vs. $V^{1/2}$ is plotted, ln(J) increases linearly up to 0.8 V; then, it deviates from the linear variation. From this fitting result, the carrier conduction at very low voltages can be explained by TE. As the voltage increases from 1.7 V to 3.8 V, α slightly increases up to 2.36. Because this value is very close to the power factor 2 corresponding to the classic SCLC model for an ideal material [27], the carrier conduction is believed to be mainly controlled by SCLC. As the voltage increases from 3.8 V to 4.7 V, the current decreases from 17 mA to 6 mA, which is known as negative differential resistance (NDR). The slope changes again to a positive value at 4.7 V. The α could be fitted to a value of about 1.13 for voltages between 4.7 to 8 V, which means that electrical conduction in this range is also governed by ohm's law. As the voltage increases further above 8 V, α increases to 2.9. Because this value is very close to the power factor 2 corresponding to the classic SCLC model for ideal material, the conduction mechanism could be SCLC. In the complete log-log plot of I-V from 0 to 20 V adapting the SCLC model, the conduction mechanism changes from ohmic to SCLC both before and after the NDR. The observed NDR can be explained on the basis of the device structure. As seen from the above TEM images (Fig. 1(c)), the ZnO NRs do not cover the PVK polymer layer completely and uniformly; thus, there is high probability that at some regions the deposited top Al electrodes are in direct contact with the PVK instead of the ZnO NRs. As a consequence, a parallel ITO/PEDOT:PSS(30 − 40 nm)/PVK (80 nm)/Al structure is formed and appears to be similar to the structure of the organic light emitting diodes (OLEDs). The NDR has been observed in many OLEDs [32–34]. Therefore the I-V curve in Fig. 2(b) can be analyzed in terms of two characteristic curves, are related to the ITO/PEDOT:PSS/ZnO NRs/Al devke and the ITO/PEDOT:PSS/Al device. In the former case, Because the energy barrier between the ZnO NR and Al electrode is as small as 0.11 eV, the I-V curve follows

ohm's law with $\alpha = 1.16$ up to a voltage 1.7 V. As can be seen in Fig. 2(b), for voltages higher than 4.7 V, the current-voltage curve is well adjusted again by another ohmic transport with $\alpha = 1.13$. It is noteworthy that the $\alpha = 1.13$ is very close to $\alpha = 1.16$ and that these two ohmic transport regions may be connected in the voltage range of 4.7 V to 8 V, represented by the dotted blue line. As the voltage increases further to higher than 8 V, the I-V curve shows the SCLC, behavior and this type of carrier transport can be understood by considering the large energy barrier of 2.19 eV at the interface between PVK (2.0 eV) and ZnO NRs (4.19 eV). This result is analogous to the previously-reported one for a organic bistable device with a ZnO NP-PMMA polymer hybrid layer [30]. In the latter case, the observed SCLC characteristics in the voltage range of 1.7 V $\sim$ 3.8 V can be attributed to another large energy barrier of 2.3 eV between PVK (2.0 eV) and Al (4.3 eV). As the voltage increases further from 3.8 to 4.7 V, the NDR dominates through the structure where Al is directly on the PVK layer with no ZnO NRs (OLED). The NDR observed in this voltage range for the first time for any devices, though it depends on the thickness of OLEDs. The cause of the NDR is not understood yet, but the current flow may be explained possibly by the model of localized pathways, which has been widely accepted in OLEDs [31]. If the exact mechanism for the observed NDR is to be as certained, further investigation with the careful analysis of the change in the spatial EL intensity is needed. Efforts were also made to fit the I-V curve (Fig. 2(b)) of our fabricated LED with a Fowler-Nordheim (F-N) tunneling model, but no good correspondence was observed. Hence, the charge transport in the fabricated Al/ZnO NR + PVK/PEDOT:PSS/ITO devices could be explained in terms of ohmic and space-charge-limited-conduction (SCLC) with no Fowler-Nordheim (F-N) tunneling.

Figure 3(a) shows room-temperature photoluminescence (PL) emission spectra of PVK, ZnO NRs, and a ZnO NR-polymer composite thin film. The PL spectra of PVK, ZnO NRs, and ZnO NR-polymer hybrid show peaks with maximum intensity at 405 nm, 400 nm, and 405 nm, respectively. The PL spectrum of the ZnO NRs can be well resolved into two peaks, are centered at around 400 nm (3.1 eV) and the other at around 437 nm (2.83 eV), depicted as two dotted peaks. The first subpeak at 3.1 eV corresponds to the near-band-gap transition of the ZnO NRs. The second subpeak at 2.83 eV corresponds to the transition related to intrinsic defects. Janotti and Van der Walle [35] and Laks *et al.* [36] correlated, the blue luminescence, at around 2.7 $\sim$ 2.9 eV to the transition from conduction band to zinc vacancies, V_{Zn}, based on the energy level and the formation energy of the ZnO intrinsic defects predicted through a first-principles calculation employing the density functional approximation (DFA) revised by the local density approximation (LDA) and the LDA+U approach. Figure 3(b) shows electroluminescence (EL) spectra taken

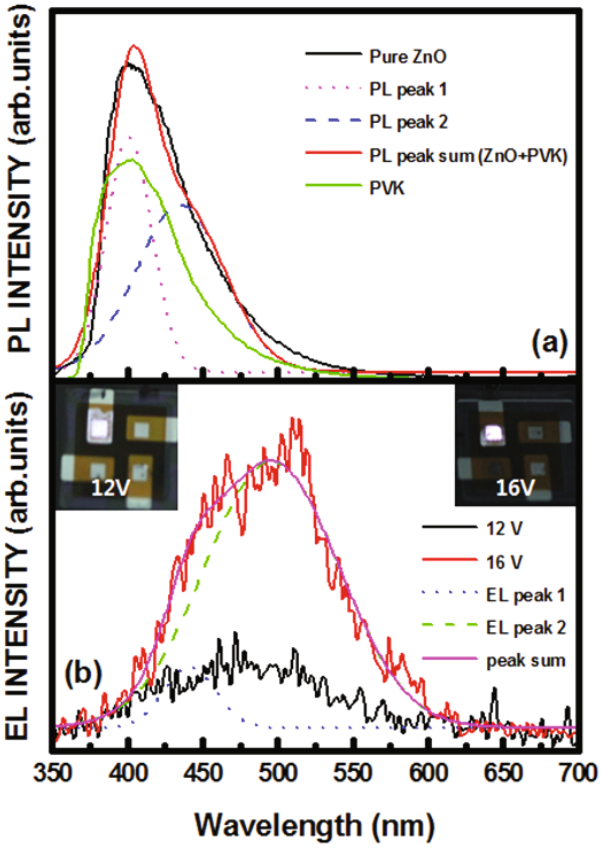

Fig. 3. (Color online) (a) PL spectra of PVK, ZnO NRs and polymer-ZnO NRs composite and (b) EL emission spectra taken at 12V and 16V applied bias. Insets: the photograph of light emission from a hybrid polymer-ZnO NRs LEDs.

at forward biases of 12 and 16 V, and the insets are corresponding pictures of the EL emission. The EL peak corresponding to 16 V can be well resolved into two small peaks with centers at 441 nm (= 2.81 eV) and 495 nm (= 2.5 eV), respectively, which exhibit red-shifts of as much as of 41 − 46 nm compared to the PL peaks.

The proposed energy level diagram of the inorganic/organic heterostructure LEDs is shown in Fig. 4(a). The PEDOT:PSS has a lowest unoccupied molecular orbital (LUMO) level and a highest occupied molecular orbital (HOMO) of 3.3 eV and 5.3 eV, respectively [37]. The highest occupied molecular orbital (HOMO) level of PVK is at approximately 5.5 eV below the vacuum level, and its lowest unoccupied molecular orbital (LUMO) level is at about 2.0 eV [38]. The valence and the conduction bands for ZnO are at 7.39 and 4.19 eV, respectively [39]. The holes, under an applied bias voltage, tunnel across the energy barrier into the valence bands of the PEDOT:PSS and the PVK. The carriers are transported through the hopping mechanism. The potential barriers for hole injection from the ITO to the HOMO level of the PEDOT:PSS and then from the HOMO level of the PVK to the valence band of the

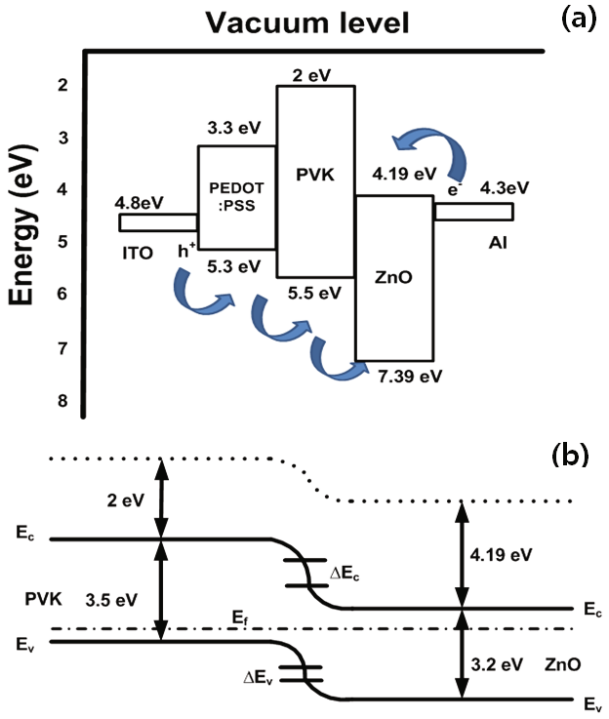

Fig. 4. (Color online) (a) Proposed energy level diagram of a hybrid Polymer-ZnO NRs LEDs. The highest occupied molecular orbital (HOMO) level and the lowest unoccupied molecular orbital (LUMO) level of PEDOT:PSS, PVK, and ZnO are taken from Ref. 37, 38, and 39. (b) The energy band diagram of p-PVK polymer/n-ZnO nanorod heterojunction.

ZnO NRs are 0.5 and 1.89 eV, respectively. The electron injection barriers between the Fermi level of the Al electrode and the conduction band of the ZnO NRs and from the conduction band of the ZnO NRs and the LUMO of the PVK are 0.11 eV and 2.19 eV, respectively.

The difference in the blue emission peaks between PL and EL can be explained through the energy band diagram of the p-PVK polymer/n-ZnO nanorod heterojunction, as shown in Fig. 4(b). The band diagram represents an ideal heterojunction for p-PVK/n-ZnO based on the Anderson model [40]. The reported electron affinity (χ) values for ZnO and PVK used for the calculations are 4.19 eV and 2 eV, respectively. The calculated band offset at the conduction band, $\Delta E_c = \chi(\mathrm{ZnO}) - \chi(\mathrm{PVK})$, $= 4.19$ eV $- 2$ eV $= 2.19$ eV and that at valance band, $\Delta E_v = \Delta E_c - \Delta E_g = 2.19$ eV $- 0.3$ eV $= 1.89$ eV. Thus, the band alignment leads to two band offsets due to the different electron affinities and the band gap values. The electrons and holes accumulate at the interface due to the conduction and the valence band offsets. The light emission due to the electron and hole recombination occurs at the interface between p-PVK and n-ZnO. In comparison with the PL peak, the observed red-shift in the position of the EL peak corresponds to about 0.29 $-$ 0.33 eV, which is very close to the difference of 0.3 eV in the band offsets.

IV. CONCLUSION

In summary, the Al/ZnO NRs +PVK/PEDOT:PSS/ITO LED device was fabricated by using a simple chemical method. The TEM images show that the hybrid PVK polymer - ZnO NR structure consists of two layers with phase segregation. The I-V characteristics can be well explained by the formation of two different LED structures of p-PVK/n-Al or p-PVK/n-ZnO NRs/Al. A NDR was observed in the I-V curve, corresponding to the regions without ZnO NRs, but the origin of this phenomenon needs further study. Carrier transport in this LED is well described by the ohmic and the SCLC mechanisms. The light emission due to electron and hole recombination occurs at the interface between the p-PVK and the the n-ZnO NRs. The shift in the blue emission peak between PL and EL of about 40 nm can be explained through band offsets by using the energy band diagram of the p-PVK polymer/n-ZnO nanorod heterojunction. These results indicate that hybrid polymer - NR composite LED, consisting of ZnO NRs dispersed in PVK, hold promise for potential applications in next-generation LED devices.

ACKNOWLEDGMENTS

The authors Dong Ick Son and Won-Kook Choi, appreciate the financial support from the KIST Institution Program [2Z04260 & 2E24871].

REFERENCES

[1] S. Coe, W.-K. Woo, M. Bawendi and V. Bulovic, Nature **420**, 800 (2002).
[2] B. O. Dabbousi and M. G. Bawendi, O. Onitsuka and M. F. Rubner, Appl. Phys. Lett. **66**, 1316 (1995).
[3] R. K. Ligman, L. Mangolini, U. R. Kortshagen and S. A. Campbel, Appl. Phys. Lett. **90**, 061116-06116-3 (2007).
[4] B. Z. Tian, X. L. Zheng, T. J. Kempa, Y. Fang, N. F. Yu, G. H. Yu, J. L. Huang and C. M. Lieber, Nature **449**, 885 (2007).
[5] O. Hayden, R. Agarwal and C. M. Lieber, Nat. Mater. **5**, 352 (2006).
[6] A. Javey, S. W. Nam, R. S. Friedman, H. Yan and C. M. Lieber, Nano Lett. **7**, 773 (2007).
[7] Y. Cui, Q. Q. Wei, H. K. Park and C. M. Lieber, Science **293**, 1289 (2001).
[8] X. W. Sun and H. S. Kwok, J. Appl. Phys. **86**, 408 (1999).
[9] M. H. Huang, S. Mao, H. Feick, H. Q. Yan, Y. Y. Wu, H. Kind, E. Weber, R. Russo and P. D. Yang, Science. **292**, 1897 (2001).
[10] J. X. Wang, X. W. Sun, Y. Yang, H. Huang, Y. C. Lee and O. K. Tan, Nanotechnology **17**, 4995 (2006).
[11] C. Y. Jiang, X. W. Sun, G. B. Lo, D. L. Kwong and J. X. Wang, Appl. Phys. Lett. **90**, 263501-263501-3 (2007).

[12] C. Li *et al.* Nanotechnology. **18**, 135604-135604-4 (2007).
[13] A. Wei, X. W. Sun, C. X. Xu, Z. L. Dong, Y. Yang, S. T. Tan and W. Huang, Nanotechnology. **17**, 1740 (2006).
[14] S. T. Tan, B. J. Chen, X. W. Sun, W. J. Fan, H. S. Kwok, X. H. Zhang and S. J. J. Chua, Appl. Phys. **98**, 013505-013505-5 (2005).
[15] Y. C. Kong, D. P. Yu, B. Zhang, W. Fang and S. Q. Feng, Appl. Phys. Lett. **78**, 407 (2001).
[16] R. Könenkamp, R. C. Word and M. Godinez, Appl. Phys. Lett. **85**, 6004 (2004).
[17] J. D. Ye, S. L. Gu, S. M. Zhu, W. Liu, S. M. Liu, R. Zhang, Y. Shi and Y. D. Zheng, Appl. Phys. Lett. **88**, 182112 (2006).
[18] A. Tsukazaki *et al.*, Nat. Mater. **4**, 42 (2005).
[19] J. H. Lim, C. K. Kang, K. K. Kim, I. K. Park, D. K. Hwang and S. J. Park, Adv. Mater. **18**, 2720 (2006).
[20] J. M. Bao, M. A. Zimmler, F. Capasso, X. W. Wang and Z. F. Ren, Nano Lett. **6**, 1719 (2006).
[21] R. Könenkamp, R. C. Word and M. Godinez, Nano Lett. **5**, 2005 (2005).
[22] A. N. Baranov, C. H. Chang, O. A. Shlyatkin, G. N. Panin, T. W. Kang and Y. J. Oh, Nanotechnology. **15**, 1613 (2004).
[23] A. N. Baranov, G. N. Panin, T. W. Kang and Y. J. Oh, Nanotechnology. **16**, 1918 (2005).
[24] D. I. Son, J. H. Kim, D. H. Park, W. K. Choi, F. Li, J. H. Ham and T. W. Kim, Nanotechnology. **19**, 055204 (2008).
[25] D. I. Son, D. H. Park, W. K. Choi and T. W. Kim, Nanotechnology. **20**, 275205-275205-6 (2009).
[26] S. M. Sze, *Physics of Semiconductor Devices*, 2nd ed. (J. Wiley & Sons, New York, 1981).
[27] K. C. Kao and W. Hwang, *Electrical Transport in Solids, International Series in the Science of Solid State*, edited by B. R. Pamplin, (Pergamon, New York, 1981), Vol. 14, p. 64.
[28] M. A. Lampert and P. Mark, *Current Injection in Solids*, (Academic, New York, 1970).
[29] H. Y.amamoto, H. Kasajima, W. Yokoyama, H. Sasabe and C. Adachi. Appl. Phys. Lett. **86**, 83502 (2005).
[30] D. I. Son, D. H. Park, W. K. Choi, S. H. Cho, W. T. Kim and T. W. Kim, Nanotechnology. **20**, 195203 (2009).
[31] S. Berlab, W. Brutting and M. Schwoever, Synthetic Metals **102**, 1034 (1999).
[32] A. Bather, I. Bleyl, C. H. Erdelen, D. Haarer, W. Paulus and H.-W. Schmidt, Adv. Mat. **13**, 1031 (1997).
[33] H. Kusano, N. Shirenishi, S. Hosaka, I. Kumara, M. Kitayama, K. Ichino and H. Kobayashi, Synth. Met. **91**, 341 (1997).
[34] H. Matoussi, L. H. Radzilowski, B. Dabbousi, E. Thomas, M. Bawendi and F. Rubner, J. Appl. Phys. **83**, 7965 (1998).
[35] A. Janotti and C. G. Van de Walle, J. Cryst. Growth. **287**, 58 (2006).
[36] D. B. Laks, C. G. Van de Walle, G. F. Neumark, P. E. Blöchl and S. T. Pantelides, Phys. Rev. B. **45**, 10965 (1992).
[37] C.-Y. Chang *et al.*, Appl. Phys. Lett. **88**, 173503 (2006).
[38] S. Chang and G. He, F. Chen, T. Gue, Y. Yang, Appl. Phys. Lett. **79**, 2088 (2001).
[39] J. M. Lin, H. Y. Lin, C. L. Cheng and Y. Fang, Nanotechnology **17**, 4391 (2006).
[40] M. Sun, Q.-F. Zhang and J.-L. Wu, J. Phys. D: Appl. Phys. **40**, 3798 (2007).